PPPL--2399

DE87 005631

THE COUPLING OF MECHANICAL DYNAMICS AND INDUCED CURRENTS IN PLATES AND SURFACES

D. W. Weissenburger and J. M. Bialek

Plasma Physics Laboratory

Princeton University

Princeton, New Jersey 08544

ABSTRACT

Significant mechanical reactions and deflections may be produced when electrical eddy currents induced in a conducting structure by transformer-like electromotive forces interact with background magnetic fields. Additional eddy currents induced by structural motion through the background fields modify both the mechanical and electrical dynamic behavior of the system. The observed effects of these motional eddy currents are sometimes referred to as magnetic damping and magnetic stiffness. This paper addresses the coupled structural deformation and eddy currents in flat plates and simple two-dimensional surfaces in three-space. A coupled system of equations has been formulated using finite element techniques for the mechanical aspects and a mesh network method for the electrical aspects of the problem.

INTRODUCTION

In connection with the design of fusion reactor components, we have previously determined that independent models of the mechanical and electrical dynamic responses of a conducting structure in a magnetic field can, in some cases, greatly overpredict the actual response of a system.[1,2] This situation is often found in the internal environment of a tokamak when a relatively small, perpendicular, magnetic field induces eddy currents by transformer action in a platelike conductor that is subjected to an essentially constant, relatively large, parallel, magnetic field. The initial eddy currents interact with the parallel field to produce Lorentz forces that move the structure, but the motion of the structure through the parallel field induces additional eddy currents that will tend to oppose the motion as prescribed by Lenz's law.

We refer to this intimate coupling of the mechanical and electrical behavior of a system as magnetomechanical coupling, however, some authors describe the same phenomena as electromagnetomechanical, electromechanical, or just magnetic coupling. Depending on the characteristics of a given system, magnetomechanical coupling can produce significant frequency shifts from the natural modes of structural vibration and also heavy damping. These effects are often referred to as magnetic stiffness and magnetic damping, respectively.

In order to improve our analytic capability, we have been developing models that include the effect of magnetomechanical coupling. Although the models can be used for general field orientations, we have been primarily interested in investigating structures subjected to a transient, perpendicular, magnetic field and a constant, parallel, magnetic field, where both external fields are assumed independent of any eddy currents in the model.

Reference 1 presents a coupled model for the rigid-body rotation of a loop or plate. Reference 2 presents a coupled model for the elastic deflection of a cantilever. For the rigid-body model it was possible to write one mechanical and one electrical equation that could be solved simultaneously. For the cantilever model the mechanical characteristics were modeled using a one-dimensional series of finite elements, and the electrical characteristics were modeled using a one-dimensional network of meshes. The coupling terms were derived so as to be consistent with both representations.

In this paper we extend our methods to a two-dimensional surface. In similarity to the cantilever, the mechanical characteristics are modeled by two-dimensional finite elements, and the electrical characteristics are modeled by a lumped-parameter mesh network. We will first derive the generalized mechanical formulation for a general system and then give specific examples of magnetomechanical coupling to an external field for the rigid-body loop/plate model, the elastic cantilever model, and an elastic rectangular plate. An additional example is given of internal magnetomechanical coupling for a model consisting of two small, coaxial loops.

GENERALIZED MECHANICS FORMULATION

Along with his many other contributions to electromagnetic science, James Clerk Maxwell pioneered the treatment of an electromechanical system with the methods of generalized mechanics.[3] We will assume that the reader is familiar with the fundamentals of this subject and not attempt a review here; however, References 4 and 5, and many other excellent texts, give detailed developments of the basic relationships that we have employed in this paper.

We will generally use the notation that brackets indicate a matrix: $[M]$; braces indicate a column vector: $\{x\}$; a diacritical dot indicates differentiation with respect to time: $\{\dot{x}\}$, $\{\ddot{x}\}$; and a superscript prime indicates a transpose: $[M]'$, $\{x\}'$.

We will consider a magnetomechanical system that is represented mechanically by a node-element model and electrically by a mesh network model that is coincident with the mechanical model. This system can be characterized by generalized coordinates:

$\{r\} = r_i$, $i = 1$ to I, where each r_i is a mechanical generalized coordinate specifying translation or rotation of the system at a node, and I is the total degrees of mechanical freedom in the system, e.g., each node has between 1 to 6 degrees of freedom $(x,y,z,\theta_x,\theta_y,\theta_z)$.

$\{q\} = q_j$, $j = 1$ to J, where each q_j is an electrical generalized coordinate specifying the electrical charge of a mesh and J is the total meshes in the system.

Additional parameters are defined in the Nomenclature Section using the same convention that i subscripts refer to mechanical coordinates and j subscripts refer to electrical coordinates.

For this system we can write the mechanical kinetic energy, the mechanical potential energy, and the magnetic potential energy as:

$$T = 1/2\ \{\dot{r}\}'\ [M]\ \{\dot{r}\}\ , \tag{1}$$

$$V = 1/2\ \{r\}'\ [K]\ \{r\}\ , \tag{2}$$

$$U = \{\Phi\}'\ \{\dot{q}\} + 1/2\ \{\dot{q}\}'\ [L]\ \{\dot{q}\}\ . \tag{3}$$

We can express the Lagrangian function for this system in its most general form without capacitive terms or internal emf sources as

$$\Lambda = T - V + U\ . \tag{4}$$

If any mechanical dissipative forces or electrical dissipative voltage drops exist, they can be expressed in vector form as

$$\{d\} = -\ [D]\ \{\dot{r}\} \tag{5}$$

and

$$\{e\} = - [R] \{\dot{q}\} . \tag{6}$$

We can then write two sets of Lagrange's equations:

$$\frac{d}{dt} \left(\frac{\partial \Lambda}{\partial \dot{r}_i}\right) - \frac{\partial \Lambda}{\partial r_i} = d_i , \quad i = 1 \text{ to } I , \tag{7}$$

and

$$\frac{d}{dt} \left(\frac{\partial \Lambda}{\partial \dot{q}_j}\right) - \frac{\partial \Lambda}{\partial q_j} = e_j , \quad j = 1 \text{ to } J . \tag{8}$$

In evaluating derivatives, we assume that [M], [K], [D], and [R] are symmetric and invariant and that [L] is symmetric and not an explicit function of time. For the moment we will consider that [L] may vary with displacement of the system as, for example, in a model consisting of two independent plates that are allowed to rotate as rigid bodies mechanically independent of each other. We can then rewrite Eqs. (7) and (8) in matrix form as

$$[M] \{\ddot{r}\} + [K] \{r\} - [C]' \{\dot{q}\} - 1/2 [E]' \{\dot{q}\} = - [D] \{\dot{r}\} \tag{9}$$

and

$$\left\{\frac{\partial \Phi}{\partial t}\right\} + [C] \{\dot{r}\} + [L] \{\ddot{q}\} + [E] \{\dot{r}\} = - [R] \{\dot{q}\} , \tag{10}$$

where we have employed the coupling matrices

$$[C] = \begin{bmatrix} \frac{\partial \Phi_1}{\partial r_1} & \frac{\partial \Phi_1}{\partial r_2} & \cdots & \frac{\partial \Phi_1}{\partial r_I} \\ \frac{\partial \Phi_2}{\partial r_1} & \frac{\partial \Phi_2}{\partial r_2} & \cdots & \frac{\partial \Phi_2}{\partial r_I} \\ \cdots & \cdots & \cdots & \cdots \\ \frac{\partial \Phi_J}{\partial r_1} & \frac{\partial \Phi_J}{\partial r_2} & \cdots & \frac{\partial \Phi_J}{\partial r_I} \end{bmatrix} \tag{11}$$

and

$$[E] = \left[\left\{\frac{\partial}{\partial r_1}[L]\{\dot{q}\}\right\} \left\{\frac{\partial}{\partial r_2}[L]\{\dot{q}\}\right\} \cdots \left\{\frac{\partial}{\partial r_I}[L]\{\dot{q}\}\right\} \right] . \tag{12}$$

We refer to [C] as the external magnetomechanical coupling matrix and to [E] as the internal magnetomechanical coupling matrix. Note that the [E] terms in Eqs. (9) and (10) are not linear, because [E] contains $\{\dot{q}\}$.

Equations (9) and (10) express in particularly powerful form the coupling relationships that must exist in any model. Although [C] and [E] multiply generalized velocity terms, they are not dissipative quantities as are [D] and [R], but enter into the system matrix in a unique manner that preserves the conservative nature of the system. The negative transpose relationship for [C] was previously noted in Ref. 2 for the cantilever beam and was also mentioned by Miya.[6] Nondissipative generalized velocity terms such as [C] are sometimes described as gyroscopic[7,8] and their interaction as gyroscopic coupling.[9] A similar negative transpose relationship with a factor of one half is observed for [E].

If one extracts [C] and [C]' independently for a given model, then the matrices can be checked to insure that they are related as above. Alternatively, if one can extract either [C] or its transpose for a given system, one can immediately write the corresponding coupling term. Similar statements can be made for [E] and [E]'.

RIGID-BODY LOOP/PLATE EXAMPLE

Figure 1 shows the basic geometry of the rigid-body, rectangular loop or plate models that are described in detail in Refs. 1 and 10. The loop or plate, lying initially in the x-y plane, is subjected to a uniform, constant B_y field and a uniform, transient B_z field, while restrained by a rotational spring. In this system the matrices [C], [D], [K], [L], [M], and [R] reduce to single, constant values and no [E] terms are present. Standard formulas were used for the loop to find the mass moment of inertia M, self-inductance L, and resistance R. Additional formulas were derived empirically for the plate using the SPARK eddy current code [11,12] with a finely meshed model to match the plate decay time constant, total current, and net torque to effective loop values of area A, inductance L, and resistance R.

We can express Eqs. (9) and (10) for this system, with θ_x = rotation angle about x axis and $\dot{q}$ = total current flowing around the loop/plate, as

$$M\ddot{\theta}_x + K\theta_x - C\dot{q} = - D\dot{\theta}_x \tag{13}$$

and

$$\frac{\partial \Phi}{\partial t} + C\dot{\theta}_x + L\ddot{q} = - R\dot{q} \ . \tag{14}$$

The net magnetic flux passing through a loop of area A is given by

$$\Phi = AB_z \cos \theta_x - AB_y \sin \theta_x \ . \tag{15}$$

Using Eq. (11) we can write for this system

$$C = \frac{\partial \Phi}{\partial \theta_x} = - AB_z \sin \theta_x - AB_y \cos \theta_x \ . \tag{16}$$

We can also write

$$\frac{\partial \Phi}{\partial t} = A\dot{B}_z \cos \theta_x - A\dot{B}_y \sin \theta_x \ . \tag{17}$$

We can calculate the Lorentz forces on the individual line elements of a rectangular loop using the relationship

$$\mathbf{F} = I\boldsymbol{\ell} \times \mathbf{B} \ , \tag{18}$$

where F is force in newtons, ℓ is length in meters, and B is a uniform magnetic field in tesla. Using Eq. (18) we find the net Lorentz torque $C\dot{q}$ on the loop about the x axis to be

$$C\dot{q} = (-AB_z \sin\theta_x - AB_y \cos\theta_x)\,\dot{q} \,. \tag{19}$$

Comparing Eqs. (16) and (19) we see that the coupling relationship checks for this system. Alternatively, we could have started with the Lagrangian function for this system,

$$\Lambda = \frac{1}{2} M \dot{\theta}_x - \frac{1}{2} K \theta^2 + \Phi \dot{q} + \frac{1}{2} L \dot{q}^2 \,. \tag{20}$$

and used Eqs. (7) and (8) to derive the magnetomechanical coupling terms along with Eqs. (13) and (14).

ELASTIC CANTILEVER EXAMPLE

Figures 2 and 3 illustrate the basic geometry of the cantilever model that is presented in detail in Ref. 2. The cantilever, lying initially in the x-z plane, is subjected to a uniform, constant B_x field and a uniform, transient B_y field. Figure 4 shows a typical displaced position of the cantilever. Each node has two degrees of freedom: y translation and θ_z rotation. The original node at the fixed end has no degrees of freedom and is not used in computations. In this system the matrices [C], [D], [K], [L], [M], and [R] are constant and no [E] terms are present.

A general element in the system consists of two nodes and one mesh, except the element at the fixed end which has only one active node. The vector of mechanical generalized coordinates, {r}, is arranged as $[y_1; \theta_{z,1}; y_2; \theta_{z,2}; \ldots y_I; \theta_{z,I}]$. Similarly, the generalized force vector is arranged as: $[F_{y,1}; \Gamma_{z,1}; F_{y,2}; \Gamma_{z,2}; \ldots F_{y,I}; \Gamma_{z,I}]$. We used standard, consistent element matrices for the mass matrix [M] and the stiffness matrix [K] that are given in Ref. 2.

The geometry of the electrical network in this example was chosen so that the self-inductances would all be identical and a simple, repetitive pattern would exist among the mutual inductances. This geometry also produces a similar relationship for the resistance matrix [R].

The self-inductance terms of [L] were calculated with the rectangular plate formula approximations that were empirically derived in the rigid-body loop/plate analysis. Mutual inductances were calculated by using the effective area formula to determine an effective dipole moment per unit current for each mesh. The mesh centroid-to-centroid distances were then used to find approximate mesh fluxes with the ideal dipole field formula.

These approximations introduce complexities into the coupling matrices and will not be used here. Instead, we assume that accurate mesh fluxes are determined by SPARK or similar code computations. Although the general deformed shape between nodes is not a flat surface, because of Gauss's divergence theorem, the net flux through an element only depends on the perimeter and not the shape of the surface, and we can choose any convenient surface for determining the flux. Thus, the external mesh flux can be expressed using the angle α shown in Fig. 4. For a general element with mesh j between node i and i+1, we can write

$$\tan \alpha = (y_{i+1} - y_i)/(x_{i+1} - x_i) \ . \tag{21}$$

Since the x_i's are constant in this system, we are only considering small deflections and the tan α can be used to approximate the sin α with the cos $\alpha = 1$. Since $A_j = a(x_{i+1}-x_i)$, the flux through the general element is

$$\Phi_j = A_j B_y - aB_x (y_{i+1} - y_i) \ . \tag{22}$$

We can also write

$$\frac{\partial \Phi_j}{\partial t} = A_j \dot{B}_y - a\dot{B}_x (y_{i+1} - y_i) \ . \tag{23}$$

Equation (22) shows that the mesh flux in this system is independent of the θ_z rotations of the nodes. Using Eq. (11) we can write row j of [C] as

$$[0; \ . \ . \ .; \ 0; \ aB_x; \ 0; \ -aB_x; \ 0; \ . \ . \ .; \ 0] \ , \tag{24}$$

where the first nonzero term occurs in column (2i). The complete matrix is shown in Table I.

In a similar manner to the rigid-body example, we can calculate the Lorentz forces on the individual line elements of a mesh using Eq. (18). For the general node i between meshes j-1 and j, we can write the net force in the y direction as

$$F_{y,i} = a\,(\dot{q}_j - \dot{q}_{j-1})\,B_x \,. \tag{25}$$

Recalling from Eq. (9) that the force vector is $[C]'\,\{\dot{q}\}$ we can write row (2i) of $[C]'$ as

$$[0;\ \ldots;\ 0;\ -aB_x;\ aB_x;\ 0,\ \ldots;\ 0]\ , \tag{26}$$

where the first nonzero term occurs in column j-1. Since no moments are produced on each line element in this uniform field example, each row (2i+1) is all zeroes. The complete matrix is shown in Table II. Comparison of Tables I and II shows that [C] is consistent with both the mechanical and electrical subsystems for this example.

ELASTIC RECTANGULAR PLATE EXAMPLE

Figure 5 shows a rectangular plate model that lies initially in the x-y plane and a general element j consisting of nodes i_1, i_2, i_3, and i_4. Each node has three degrees of freedom: z translation, θ_x rotation, and θ_y rotation. This system must be constrained at one or more nodes to have a well-defined mechanical set of equations. The plate is subjected to B_x, B_y, and B_z fields. We will allow B_z to be uniform in space, but time-varying, B_x and B_y will be constant in time and they can vary linearly with x or y. In this system the matrices [C], [D], [K], [L], [M], and [R] are constant and no [E] terms are present.

We arrange the mechanical generalized coordinates as

$$\{r\} = [z_1;\theta_{x,1};\theta_{y,1};z_2;\theta_{x,2};\theta_{y,2};\ \ldots\ z_I;\theta_{x,I};\theta_{y,I}]' \tag{27}$$

and the generalized force vector as

$$\{F\} = [F_{z,1};\Gamma_{x,1};\Gamma_{y,1};F_{z,2};\Gamma_{x,2};\Gamma_{y,2};\ \ldots\ F_{z,I};\Gamma_{x,I};\Gamma_{y,I}]' \,. \tag{28}$$

Standard, consistent [M] and [K] representations for this element can be found in Ref. 13.

It is possible to modify the method used to calculate the [L] and [R] values for the cantilever, if a similar, regular mesh is chosen. However, for a general mesh network, Step 1 of the SPARK code produces [L] and [R] in a straightforward manner. Other similar network mesh codes may also be suitable for this purpose. SPARK calculates mutual inductances by numerically integrating the magnetic vector potential around a mesh. This can produce slight, artificial asymmetries in [L], but a symmetric matrix can be obtained by averaging [L] and [L]'. A symmetric [R] is always produced by SPARK.

We will consider the submatrix of [C] for one general element. The complete matrix can be generated by the addition of the submatrices for all the elements. In general we will have forces and moments at each node of an element. We will calculate nodal loads using the work-equivalent load method.[14,15] We have previously used this technique to produce nodal loads with the SPARK code.

In conformity with the electrical model, we assume that electrical currents only flow in the branch lines between nodes. The branches form the boundaries of the mechanical elements and, thus, the Lorentz forces only appear on the element boundaries. On the boundaries of the plate element of Ref. 13 the shape functions reduce to cubic polynomials that are identical to the shape functions for a simple beam.[16,17] We will refer to the beam shape functions directly in our following analysis.

Ignoring in-plane loads, since we only allow z deformation, we will determine the concentrated moments and forces that when applied to the nodes of a branch produce the same work as the total distributed load along the branch. A branch of length ℓ is described using the coordinate s that starts at node 1 with the value 0 and ends at node 2 with the value ℓ. The usual Hermitian shape functions for a general branch are

$$\begin{Bmatrix} N_{z1}(s) \\ N_{\theta 1}(s) \\ N_{z2}(s) \\ N_{\theta 2}(s) \end{Bmatrix} = \begin{Bmatrix} 1 - 3s^2/\ell^2 + 2s^3/\ell^3 \\ s - 2s^2/\ell + s^3/\ell^2 \\ 3s^2/\ell^2 - 2s^3/\ell^3 \\ -s^2/\ell + s^3/\ell^2 \end{Bmatrix} . \tag{29}$$

For a distributed transverse load w(s) along a branch, the equivalent nodal loads are given by

$$\begin{Bmatrix} F_1 \\ \Gamma_1 \\ F_2 \\ \Gamma_2 \end{Bmatrix} = \begin{Bmatrix} \int_0^\ell w(s)N_{z1}(s)ds \\ \int_0^\ell w(s)N_{\theta 1}(s)ds \\ \int_0^\ell w(s)N_{z2}(s)ds \\ \int_0^\ell w(s)N_{\theta 2}(s)ds \end{Bmatrix} . \tag{30}$$

In this system the direction of the moments is given by the cross product of the vector from node 1 to node 2 into a vector in the direction of positive loads. For the branch $(i_1; i_2)$ of the general mesh with $\ell = x_2 - x_1$, the Lorentz distributed load is given by

$$w(s) = \{[B_y(i_2)-B_y(i_1)]s/\ell + B_y(i_1)\}\, \mathring{q}_j . \tag{31}$$

Evaluating the integrals in Eq. 30 we get

$$\begin{Bmatrix} F_z(i_1) \\ \Gamma_x(i_1) \\ \Gamma_y(i_1) \\ F_z(i_2) \\ \Gamma_x(i_2) \\ \Gamma_y(i_2) \end{Bmatrix} = \mathring{q}_j \begin{Bmatrix} (\ell/20)[7B_y(i_1)+3B_y(i_2)] \\ 0 \\ (-\ell^2/60)[3B_y(i_1)+2B_y(i_2)] \\ (\ell/20)[3B_y(i_1)+7B_y(i_2)] \\ 0 \\ (\ell^2/60)\ [2B_y(i_1)+3B_y(i_2)] \end{Bmatrix} . \tag{32}$$

Similar expressions to Eq. (32) can be derived for the other three branches of the general mesh. Summing the branch results and dividing by $\dot{q}_j$ gives the nonzero values in column j of [C]' in Eq. (9). The net result for the general mesh is given in Table III.

Direct evaluation of [C] in Eq. (10) can be done by recalling Gauss's divergence theorem. The original perimeter of the general mesh is deformed as its member branches are deflected, but we can describe a general branch deflection with the shape functions in Eq. (29) as

$$z(s) = [N_{z1}(s),\ N_{\theta 1}(s),\ N_{z2}(s),\ N_{\theta 2}(s)] \begin{Bmatrix} z_1 \\ \theta_1 \\ z_2 \\ \theta_2 \end{Bmatrix} \tag{33}$$

Since [C] consists of the spatial derivatives of the mesh fluxes, the original perimeter can be neglected and only the variable flux produced by the branch deformations evaluated. For a general branch this flux is

$$\Delta\Phi = \int_0^{\ell} B(s)z(s)ds\ , \tag{34}$$

where B(s) is the magnetic field normal to the area mapped out by the beam deformation.

Consideration of Eq. (31) for branch $(i_1;\ i_2)$ of the general mesh shows that, *in general*,

$$B(s) = w(s)/\dot{q}_j\ . \tag{35}$$

Taking the time derivative of Eq. (34) and using Eqs. (30), (33), and (35) we get

$$\dot{\Delta\Phi} = \frac{1}{\dot{q}_j} [F_1,\ r_1,\ F_2,\ r_2] \begin{Bmatrix} \dot{z}_1 \\ \dot{\theta}_1 \\ \dot{z}_2 \\ \dot{\theta}_2 \end{Bmatrix}. \tag{36}$$

The row vector divided by $\dot{q}_j$ in Eq. (36) corresponds exactly to the branch contribution to column j in [C]'. As with Eq. (32) we can derive similar expressions to Eq. (36) for each branch of the general mesh. Summing the branch results gives us the nonzero elements in row j of [C]. Thus, for each branch of every mesh we get an exact correspondence between a row of [C] and a column of [C]'as desired. We note that this result does not depend on the particular degrees of freedom or shape functions chosen for this example. A similar correspondence can be shown for each degree of freedom of a general element.

TWO SMALL, CIRCULAR, COAXIAL LOOPS EXAMPLE

Since all the other examples demonstrate the external magnetomechanical coupling matrix [C] and have no internal magnetomechanical coupling matrix [E], in the interest of completeness, we give an example here that has only an [E] and no [C]. Figure 6 shows two small, circular, filamentary coils located coaxially on the z axis. The symmetry of the system allows us to use the cylindrical coordinate ρ for radial position from the z axis. We assume that the coils are located far enough apart to allow the magnetic field from each coil to be determined using a dipole field approximation.

Coil 1 carries current $\dot{q}_1$, has a radius of a_1, and is allowed to move only along z restrained by a linear spring constant k_1 about equilibrium position z_1. Coil 2 carries current $\dot{q}_2$, has a radius of a_2, and is allowed to move only along z restrained by a linear spring constant k_2 about equilibrium position z_2.

The magnetic flux through coil 1 due to coil 2 is given by

$$\Phi(1,2) = 1/2\ \mu_0 \pi\ a_1^2\ a_2^2\ \dot{q}_2\ (z_2-z_1)^{-3}\ , \tag{37}$$

and the magnetic flux through coil 2 due to coil 1 is given by

$$\Phi(2,1) = 1/2\ \mu_0 \pi\ a_1^2\ a_2^2\ \dot{q}_1\ (z_2-z_1)^{-3}\ . \tag{38}$$

Using Gauss's divergence theorem we can calculate the radial fields at coil 1 and coil 2 as

$$B_\rho(1,2) = \frac{-1}{2\pi a_1}\frac{\partial\Phi(1,2)}{\partial z_1} = -3/4\ \mu_o\ a_1\ a_2^2\ \dot{q}_2\ (z_2-z_1)^{-4} \tag{39}$$

and

$$B_\rho(2,1) = \frac{-1}{2\pi a_2}\frac{\partial\Phi(2,1)}{\partial z_2} = +3/4\ \mu_o\ a_1^2\ a_2\ \dot{q}_1\ (z_2-z_1)^{-4}\ . \tag{40}$$

The forces on coil 1 and coil 2 are then given by

$$\begin{Bmatrix} F_z(1,2) \\ F_z(2,1) \end{Bmatrix} = \begin{Bmatrix} -2\pi a_1\ \dot{q}_1 B_\rho(1,2) \\ -2\pi a_2\ \dot{q}_2 B_\rho(2,1) \end{Bmatrix} = \begin{Bmatrix} 3/2\mu_o\pi a_1^2 a_2^2 \dot{q}_1\dot{q}_2(z_2-z_1)^{-4} \\ -3/2\mu_o\pi a_1^2 a_2^2 \dot{q}_1\dot{q}_2(z_2-z_1)^{-4} \end{Bmatrix}\ . \tag{41}$$

Similarly, the spatially dependent flux derivative term in Eq. (10) is given by

$$[E]\begin{Bmatrix} \dot{z}_1 \\ \dot{z}_2 \end{Bmatrix} = \begin{bmatrix} \frac{\partial\Phi(1,2)}{\partial z_1} & \frac{\partial\Phi(1,2)}{\partial z_2} \\ \frac{\partial\Phi(2,1)}{\partial z_1} & \frac{\partial\Phi(2,1)}{\partial z_2} \end{bmatrix}\begin{Bmatrix} \dot{z}_1 \\ \dot{z}_2 \end{Bmatrix}\ . \tag{42}$$

Evaluating [E] in Eq. (42) we get

$$[E] = \frac{\mu_o\pi a_1^2 a_2^2}{(z_2-z_1)^4}\begin{bmatrix} 3/2\ \dot{q}_2 & -3/2\ \dot{q}_2 \\ 3/2\ \dot{q}_1 & -3/2\ \dot{q}_1 \end{bmatrix}\ . \tag{43}$$

It is readily checked that the force term in Eq. (9) agrees with Eq. (41):

$$\begin{Bmatrix} F_z(1,2) \\ F_z(2,1) \end{Bmatrix} = 1/2\ [E]\begin{Bmatrix} \dot{q}_1 \\ \dot{q}_2 \end{Bmatrix}\ . \tag{44}$$

Since the inductance terms are just magnetic flux per unit current and the self-inductances are constant values, we could also have found [E] by using Eq. (12).

EXTENSIONS TO MORE COMPLICATED SURFACES

The basic technique described in the examples of converting distributed branch transverse loads to equivalent nodal loads is equally applicable to nonrectangular elements and nonflat surfaces or 3-D networks. In fact, Step 5 of the SPARK code already produces three fluxes and three moments in the global coordinate system at each node of an arbitrary surface of triangles and/or quadrilaterals. SPARK also generates [L] and [R] for this system, however, no magnetomechanical coupling is employed.

When using an electrical mesh network method some topological considerations must be taken into account that have no mechanical counterpart. Surface holes must be included as electrical meshes, and nonplanar topologies, such as a sphere or torus, require special electrical loops. Fortunately, these procedures do not effect the mechanical equations. Nevertheless, finding an appropriate element for a particular surface along with its mass and stiffness matrices can be difficult.

Even relatively small coupled problems require large amounts of computer storage. The [C], [D], [K], [M], and [R] matrices are generally sparse while [E] and [L] are generally dense. The most efficient solution techniques for large problems are machine dependent. Trade-offs in problem size versus solution speed are necessary even on supercomputers.

CONCLUSION

Conducting structures in magnetic fields have been modeled with generalized coordinates as systems of equations that include the magnetomechanical coupling terms. For a given model, mechanical aspects have been formulated using a finite element method, and electrical aspects have been formulated using a mesh network method. Coupling terms have been derived using techniques consistent with both methods. The matrix of mechanical coupling terms has been shown to be readily derivable from the matrix of

electrical coupling terms and vice versa. For external field coupling, a negative transpose relationship exists between the matrices. For internal field coupling an additional factor of one half is required.

ACKNOWLEDGEMENT

This work was supported by U.S. Department of Energy Contract No. DE-AC02-76-CHO-3073.

NOMENCLATURE

A = area (m^2).

$[C]$ = external magnetomechanical coupling matrix (J × I): (Wb/m).

$[D]$ = mechanical damping matrix (I × I) (N-s/m or N-m-s/rad).

d_i = mechanical dissipative force (N or N-m).

$[E]$ = internal magnetomechanical coupling matrix (J × I): (Wb/m).

e_j = electrical dissipative voltage drop (V)

F = mechanical force (N).

I = total degrees of mechanical freedom in system.

J = total meshes in system.

$[K]$ = mechanical stiffness matrix (I × I); (N/m or N-m/rad).

$[L]$ = mesh inductance matrix (J × J); (H).

ℓ = branch length (m).

$[M]$ = mass matrix (I × I); (kg or kg-m^2/rad).

N = shape function (dimensionless).

q_j = electrical generalized coordinate (C).

$[R]$ = mesh resistance matrix (J × J); (Ω).

r_i = mechanical generalized coordinate (m or rad).

s = local branch coordinate (m).

t = time (s).

T = mechanical kinetic energy (J).

U = magnetic potential energy (J).

V = mechanical potential energy (J).

$w(s)$ = local distributed transverse loading function (N/m).

x,y,z = rectangular coordinates (m).

Γ = mechanical moment (N-m).

$\theta_x,\theta_y,\theta_z$ = angle of rotation about x,y,z axes, respectively (rad).

Λ = Lagrangian function (J).

Φ_j = external magnetic flux through mesh (Wb).

REFERENCES

1. J. BIALEK, D. WEISSENBURGER, M. ULRICKSON, and J. CECCHI, "Modeling the Coupling of Magnetodynamics and Elastomechanics in Structural Analysis," in Proc. 10th Symp. Fusion Engineering, Philadelphia, Pennsylvania, December 5-9, 1983, IEEE Conf. 83-CH1916-6, p. 51, Institute of Electrical and Electronics Engineers.

2. J. M. BIALEK and D. W. WEISSENBURGER, "The Coupling of Mechanical Dynamics and Induced Currents in a Cantilever Beam," in Proc. Workshop on Computational Electromagnetics, Pittsburgh, Pennsylvania, December, 1984, p. 193, Z. J. CENDES, Ed., International Association for Mathematics and Computers in Simulation.

3. JAMES CLERK MAXWELL, A Treatise on Electricity and Magnetism, 3rd ed., Part IV, Chapters 5-7, Clarendon Press, Oxford, England (1892), reprinted Dover, New York (1954).

4. HARRY J. WHITE and SELMO TAUBER, Systems Analysis, Chapters 6-8, W. B. Saunders, Philadelphia (1969).

5. DARE A. WELLS, Lagrangian Dynamics, McGraw-Hill, New York (1967).

6. KENZO MIYA and MITSURU VESAKA, "An Application of Finite Element Method to Magnetomechanics of Superconducting Magnets for Magnetic Fusion Reactors," Nucl. Eng. Design, 72, 275 (1982).

7. ARNOLD SOMMERFELD, Mechanics, 4th ed., p. 169, MARTIN O. STERN, Transl., Academic Press, New York (1952).

8. WHITE and TAUBER, op. cit., p. 285.

9. ROBERT H. CANNON, JR., Dynamics of Physical Systems, p. 620. McGraw-Hill, New York (1967).

10. D. W. WEISSENBURGER, J. M. BIALEK, G. J. CARGULIA, M. ULRICKSON, M. J. KNOTT, L. R. TURNER, and R. B. WEHRLE, "Experimental Observations of the Coupling Between Induced Currents and Mechanical Motion in Torsionally Supported Square Loops and Plates," Fusion Technol. (in press).

11. D. W. WEISSENBURGER and J. M. BIALEK, "An Interface Between Eddy Current Calculation and Structural Analysis," IEEE Trans. Magn., MAG-19, 2619 (1983).

12. D. W. WEISSENBURGER, "SPARK Version One: Reference Manual," Princeton University, Plasma Physics Laboratory Report PPPL-2040 (1983) 76 pp.

13. O. C. ZIENKIEWICZ, The Finite Element Method, 3rd ed., pp. 234-240; p. 535, McGraw-Hill, New York (1977).

14. HARRY G. SCHAEFFER, MSC/NASTRAN Primer: Static and Normal Modes Analysis, pp. 101-103, Schaeffer Analysis, Mount Vernon, New Hampshire (1977).

15. T. Y. YANG, Finite Element Structural Analysis, pp. 143-146, Prentice-Hall, Englewood Cliffs, New Jersey (1986).

16. CHANDRAKANT S. DESAI, Elementary Finite Element Method, pp. 377-378, Prentice-Hall, Englewood Cliffs, New Jersey (1979).

17. R.K. LIVESLY, Finite Elements: An Introduction for Engineers, p. 156, Cambridge University, Cambridge, England (1983).

TABLE I

MATRIX [C] FOR CANTILEVER EXAMPLE

$$(aB_x)\begin{bmatrix}
-1 & 0 & 0 & 0 & 0 & & & & & & \\
+1 & 0 & -1 & 0 & 0 & & & & & & \\
0 & 0 & +1 & 0 & -1 & & & & & & \\
0 & 0 & 0 & 0 & +1 & & & & & & \\
 & & & & & \ddots & & & & & \\
 & & & & & & \ddots & & & & \\
 & & & & & & & -1 & 0 & 0 & 0 & 0 & 0 \\
 & & & & & & & +1 & 0 & -1 & 0 & 0 & 0 \\
 & & & & & & & 0 & 0 & +1 & 0 & -1 & 0
\end{bmatrix}$$

TABLE II

MATRIX [C]' FOR CANTILEVER EXAMPLE.

$$(aB_x)\begin{bmatrix}
-1 & +1 & 0 & 0 & & & & & & & & \\
0 & 0 & 0 & 0 & & & & & & & & \\
0 & -1 & +1 & 0 & & & & & & & & \\
0 & 0 & 0 & 0 & & & & & & & & \\
 & & & & \ddots & & & & & & & \\
 & & & & & \ddots & & & & & & \\
 & & & & & & \ddots & & & & & \\
 & & & & & & & 0 & -1 & +1 & 0 \\
 & & & & & & & 0 & 0 & 0 & 0 \\
 & & & & & & & 0 & 0 & -1 & +1 \\
 & & & & & & & 0 & 0 & 0 & 0 \\
 & & & & & & & 0 & 0 & 0 & -1 \\
 & & & & & & & 0 & 0 & 0 & 0
\end{bmatrix}$$

TABLE III

NONZERO ELEMENTS OF COLUMN j OF [C]' FOR THE RECTANGULAR PLATE EXAMPLE

$$
(1/\dot{q}_j)\begin{Bmatrix} F_z(i_1) \\ \Gamma_x(i_1) \\ \Gamma_y(i_1) \\ F_z(i_2) \\ \Gamma_x(i_2) \\ \Gamma_y(i_2) \\ F_z(i_3) \\ \Gamma_x(i_3) \\ \Gamma_y(i_3) \\ F_z(i_4) \\ \Gamma_x(i_4) \\ \Gamma_y(i_4) \end{Bmatrix} = (1/20)\begin{bmatrix}
7\ell_4 & 7\ell_1 & & 3\ell_1 & & & 3\ell_4 & \\
\ell_4^2 & & & & & & 2\ell_4^2/3 & \\
 & -\ell_1^2 & & -2\ell_1^2/3 & & & & \\
 & 3\ell_1 & -7\ell_2 & 7\ell_1 & -3\ell_2 & & & \\
 & & -\ell_2^2 & & -2\ell_2^2/3 & & & \\
 & 2\ell_1^2/3 & & \ell_1^2 & & & & \\
 & & -3\ell_2 & & -7\ell_2 & -7\ell_3 & & -3\ell_3 \\
 & & 2\ell_2^2/3 & & \ell_2^2 & & & \\
 & & & & & -\ell_3^2 & & -2\ell_3^2/3 \\
3\ell_4 & & & & & -3\ell_3 & 7\ell_4 & -7\ell_3 \\
-2\ell_4^2/3 & & & & & & -\ell_4^2 & \\
 & & & & & 2\ell_3^2/3 & & \ell_3^2
\end{bmatrix}\begin{Bmatrix} B_x(i_1) \\ B_y(i_1) \\ B_x(i_2) \\ B_y(i_2) \\ B_x(i_3) \\ B_y(i_3) \\ B_x(i_4) \\ B_y(i_4) \end{Bmatrix}
$$

where: $\ell_1 = x(i_2) - x(i_1)$

$\ell_2 = y(i_3) - y(i_2)$

$\ell_3 = x(i_3) - x(i_4)$

$\ell_4 = y(i_4) - y(i_1)$

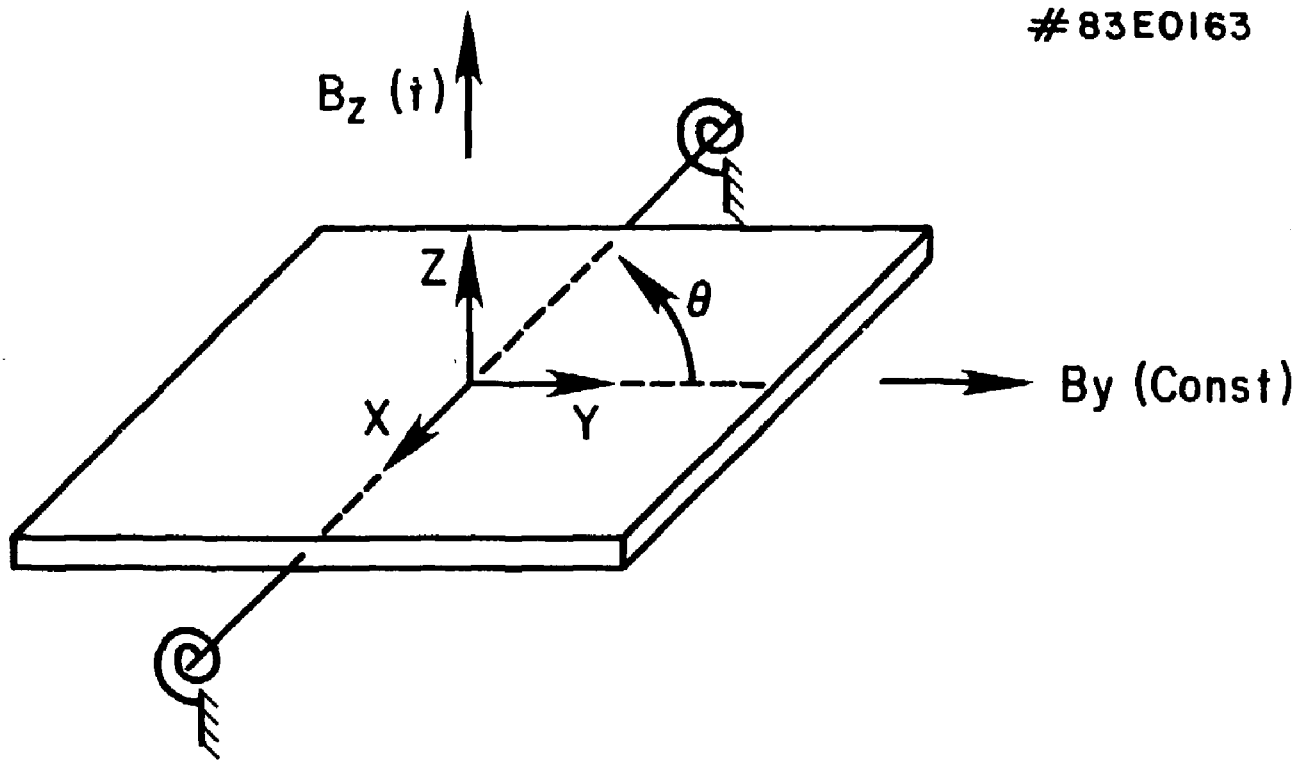

Fig. 1. Rigid-body, rotating loop/plate example.

#84E0142

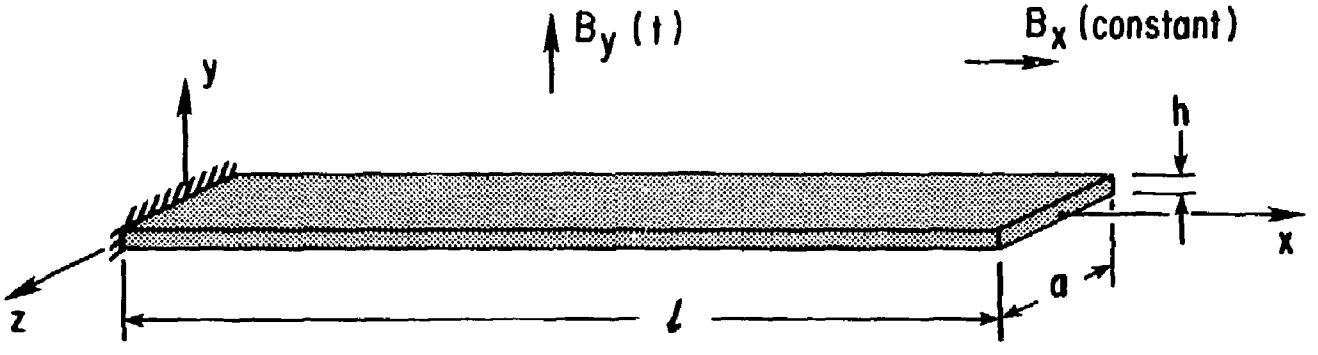

Fig. 2. Basic cantilever beam model.

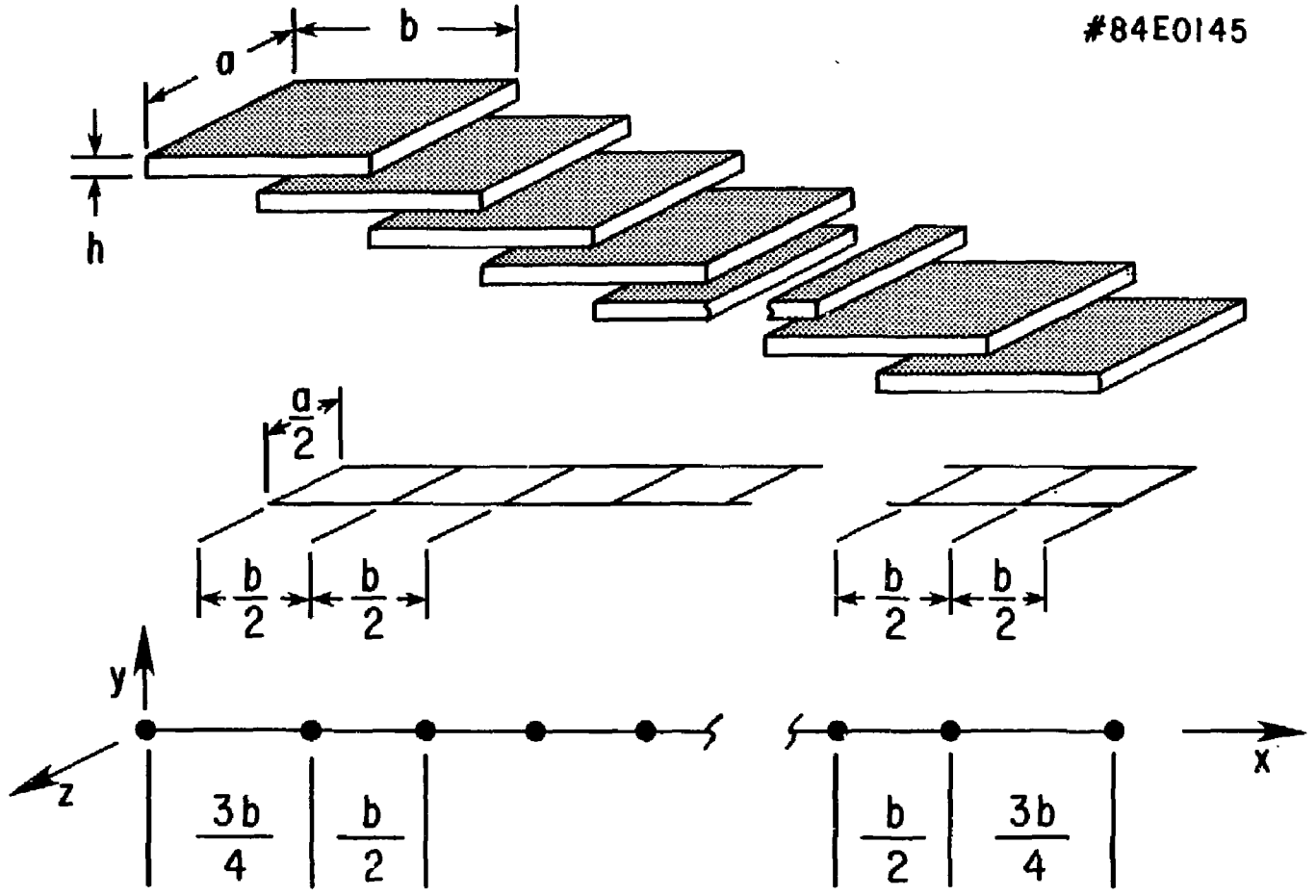

Fig. 3. Illustrative problem characterizations: overlapping electrical meshes (top), electrical branch network (middle), and mechanical beam series (bottom).

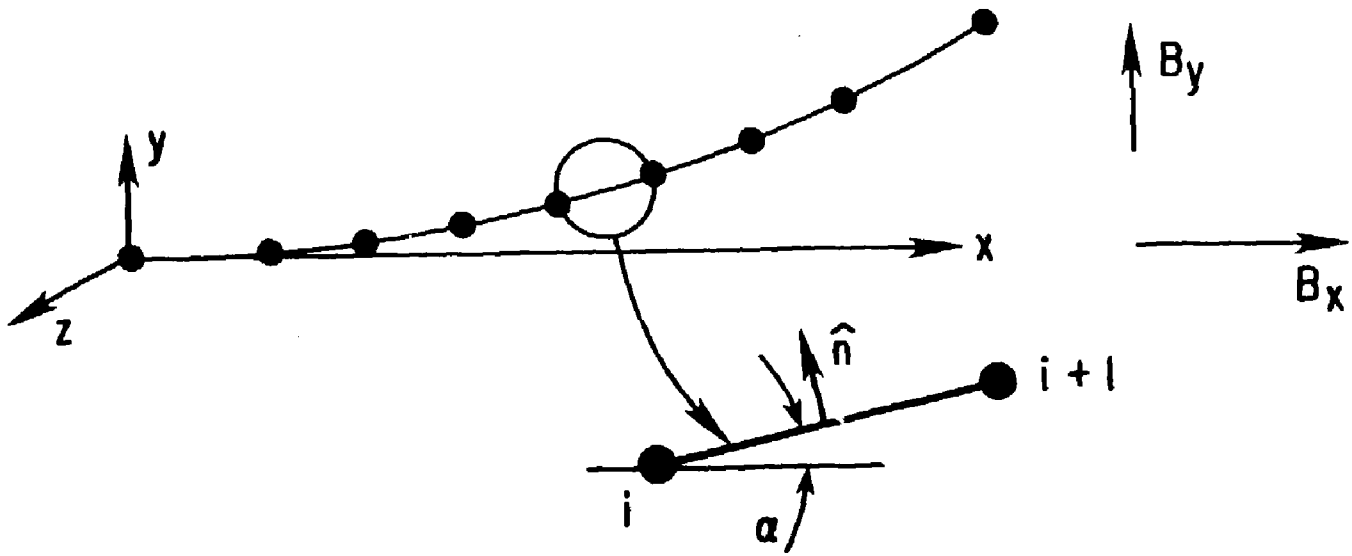

Fig. 4. Example of a deflected beam with detail of typical mesh/panel element.

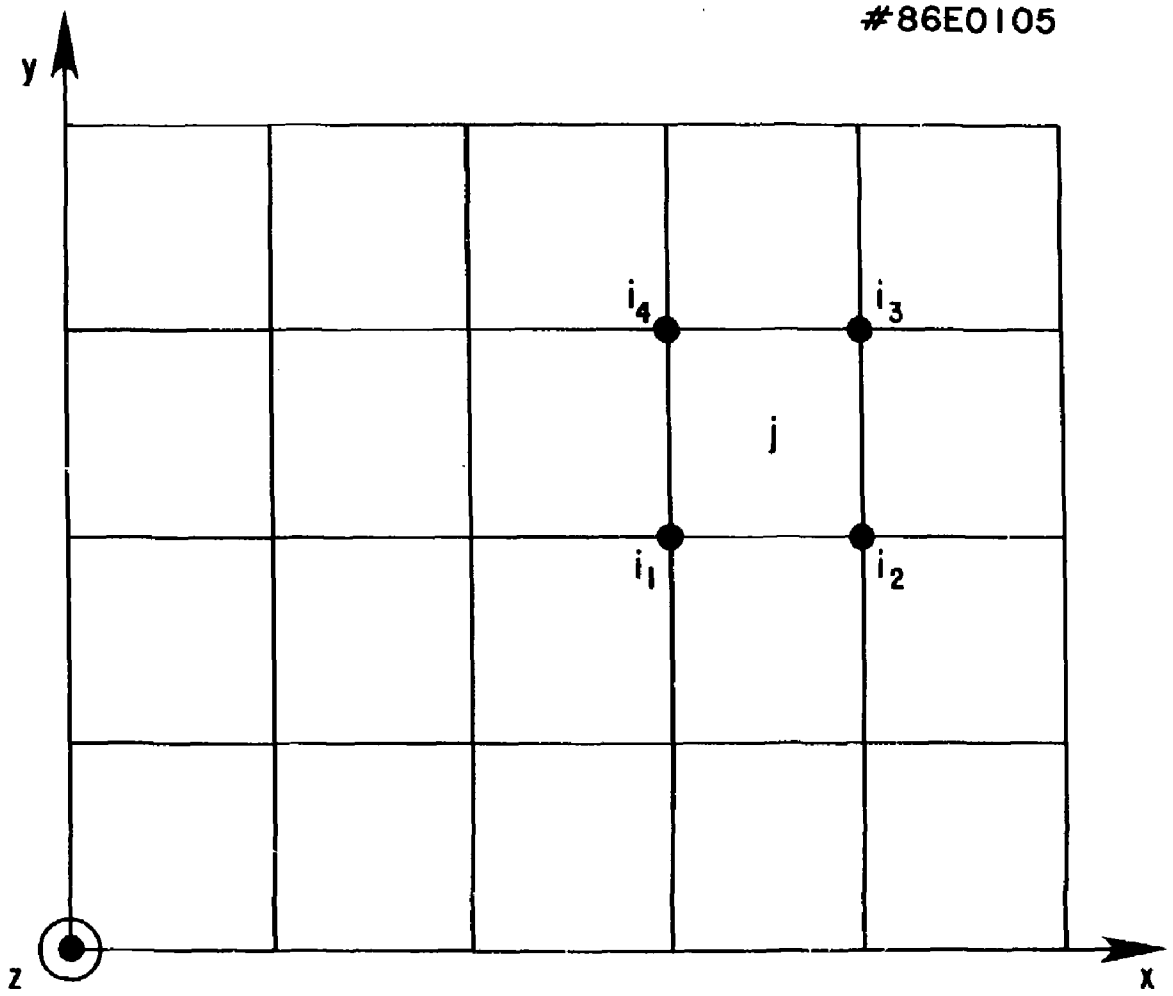

Fig. 5. Rectangular plate example with typical mesh j consisting of nodes: i_1, i_2, i_3, and i_4.

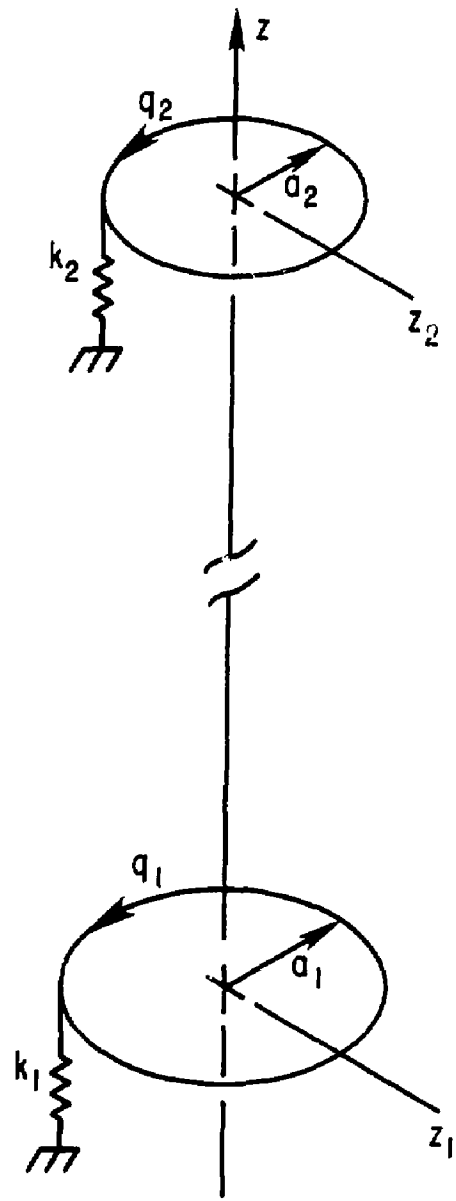

Fig. 6. Two small, coaxial, circular loops example.

EXTERNAL DISTRIBUTION IN ADDITION TO UC-20

Plasma Res Lab, Austra Nat'l Univ, AUSTRALIA
Dr. Frank J. Paoloni, Univ of Wollongong, AUSTRALIA
Prof. I.R. Jones, Flinders Univ., AUSTRALIA
Prof. M.H. Brennan, Univ Sydney, AUSTRALIA
Prof. F. Cap, Inst Theo Phys, AUSTRIA
M. Goossens, Astronomisch Instituut, BELGIUM
Prof. A. Boucique, Laboratorium voor Natuurkunde, BELGIUM
Dr. D. Palumbo, Dg XII Fusion Prog, BELGIUM
Ecole Royale Militaire, Lab de Phys Plasmas, BELGIUM
Dr. P.H. Sakanaka, Univ Estadual, BRAZIL
Lib. & Doc. Div., Instituto de Pesquisas Espaciais, BRAZIL
Dr. C.R. James, Univ of Alberta, CANADA
Prof. J. Teichmann, Univ of Montreal, CANADA
Dr. H.M. Skarsgard, Univ of Saskatchewan, CANADA
Prof. S.R. Sreenivasan, University of Calgary, CANADA
Prof. Tudor W. Johnston, INRS-Energie, CANADA
Dr. Hannes Barnard, Univ British Columbia, CANADA
Dr. M.P. Bachynski, MPB Technologies, Inc., CANADA
Chalk River, Nucl Lab, CANADA
Zhangwu Li, SW Inst Physics, CHINA
Library, Tsing Hua University, CHINA
Librarian, Institute of Physics, CHINA
Inst Plasma Phys, Academia Sinica, CHINA
Dr. Peter Lukac, Komenskeho Univ, CZECHOSLOVAKIA
The Librarian, Culham Laboratory, ENGLAND
Prof. Schatzman, Observatoire de Nice, FRANCE
J. Radet, CEN-BP6, FRANCE
JET Reading Room, JET Joint Undertaking, ENGLAND
AM Dupas Library, AM Dupas Library, FRANCE
Dr. Tom Mual, Academy Bibliographic, HONG KONG
Preprint Library, Cent Res Inst Phys, HUNGARY
Dr. R.K. Chhajlani, Vikram Univ, INDIA
Dr. B. Dasgupta, Saha Inst, INDIA
Dr. P. Kaw, Physical Research Lab, INDIA
Dr. Phillip Rosenau, Israel Inst Tech, ISRAEL
Prof. S. Cuperman, Tel Aviv University, ISRAEL
Prof. G. Rostagni, Univ Di Padova, ITALY
Librarian, Int'l Ctr Theo Phys, ITALY
Miss Clelia De Palo, Assoc EURATOM-ENEA, ITALY
Biblioteca, del CNR EURATOM, ITALY
Dr. H. Yamato, Toshiba Res & Dev, JAPAN
Direc. Dept. Lg. Tokamak Dev. JAERI, JAPAN
Prof. Nobuyuki Inoue, University of Tokyo, JAPAN
Research Info Center, Nagoya University, JAPAN
Prof. Kyoji Nishikawa, Univ of Hiroshima, JAPAN
Prof. Sigeru Mori, JAERI, JAPAN
Prof. S. Tanaka, Kyoto University, JAPAN
Library, Kyoto University, JAPAN
Prof. Ichiro Kawakami, Nihon Univ, JAPAN
Prof. Satoshi Itoh, Kyushu University, JAPAN
Dr. D.I. Choi, Adv. Inst Sci & Tech, KOREA
Tech Info Division, KAERI, KOREA
Bibliotheek, Fom-Inst Voor Plasma, NETHERLANDS
Prof. B.S. Liley, University of Waikato, NEW ZEALAND
Prof. J.A.C. Cabral, Inst Superior Tecn, PORTUGAL
Dr. Octavian Petrus, ALI CUZA University, ROMANIA
Prof. M.A. Hellberg, University of Natal, SO AFRICA
Dr. Johan de Villiers, Plasma Physics, Nucor, SO AFRICA
Fusion Div. Library, JEN, SPAIN
Prof. Hans Wilhelmson, Chalmers Univ Tech, SWEDEN
Dr. Lennart Stenflo, University of UMEA, SWEDEN
Library, Royal Inst Tech, SWEDEN
Centre de Recherchesen, Ecole Polytech Fed, SWITZERLAND
Dr. V.T. Tolok, Kharkov Phys Tech Ins, USSR
Dr. D.D. Ryutov, Siberian Acad Sci, USSR
Dr. G.A. Eliseev, Kurchatov Institute, USSR
Dr. V.A. Glukhikh, Inst Electro-Physical, USSR
Institute Gen. Physics, USSR
Prof. T.J.M. Boyd, Univ College N Wales, WALES
Dr. K. Schindler, Ruhr Universitat, W. GERMANY
ASDEX Reading Rm, IPP/Max-Planck-Institut fur Plasmaphysik, F.R.G.
Nuclear Res Estab, Julich Ltd, W. GERMANY
Librarian, Max-Planck Institut, W. GERMANY
Bibliothek, Inst Plasmaforschung, W. GERMANY
Prof. R.K. Janev, Inst Phys, YUGOSLAVIA